

IEEE © 2026. Personal use of this material is permitted. Permission from IEEE must be obtained for all other uses, including reprinting/republishing this material for advertising or promotional purposes, collecting new collected works for resale or redistribution to servers or lists, or reuse of any copyrighted component of this work in other works. This work has been submitted to the IEEE for possible publication. Copyright may be transferred without notice, after which this version may no longer be accessible.

# Adaptive Modular Geometric Control of Robotic Manipulators

Mahdi Hejrati, Amir Hossein Barjini, Gokhan Alcan, and Jouni Mattila

**Abstract**—This paper proposes an adaptive modular geometric control framework for robotic manipulators. The proposed methodology decomposes the overall manipulator dynamics into individual modules, enabling the design of local geometric control laws at the module level. To address parametric uncertainties, a geometric adaptive law is incorporated into the control structure. The adaptation mechanism updates only the spatial inertia parameters using a single adaptation gain for the entire system, while guaranteeing physically consistent and drift-free parameter estimates. Numerical simulations are provided to validate the effectiveness of the proposed approach in comparison to the existing modular and geometric methods.

## I. INTRODUCTION

Over the past two decades, geometric control on Lie groups has demonstrated substantial advantages in modeling, control, estimation, and learning for multi-body systems. Foundational developments such as PD control on the Euclidean group [1] were followed by intrinsic control designs on  $SE(3)$ , including quadrotor control [2] and geometric impedance control for manipulators [3]. A key strength of the geometric framework lies in its unified treatment of position and orientation errors, in contrast to conventional Cartesian approaches that handle them separately. This intrinsic representation not only improves tracking performance but also enhances learning-based methods success rate, as shown in [4]. Beyond control, geometric principles have been successfully applied to inertial parameter identification [5], [6] with adaptation laws that ensure physical consistency [7], as well as trajectory optimization on manifolds [8]. Collectively, these results highlight the effectiveness of differential geometric formulations for interconnected multi-body systems.

Modularity is a favorable and scalable design paradigm for complex robotic systems, enabling subsystem-level design, reduced computational burden, structural flexibility, and systematic stability analysis. A prominent realization of this philosophy is virtual decomposition control (VDC) [9], which decomposes a multi-body system into dynamically consistent subsystems interconnected through virtual power flows. VDC has demonstrated high-performance precision control for modular robots [10] and has undergone continued theoretical development, including subsystem-based observer–controller duality [11], extensions to strict-feedback structures [12], and practical implementations with robustness guarantees on complex robotic platforms [13]–[15]. These developments establish VDC as an efficient and scalable framework for highly interconnected multi-body systems.

Motivated by these advantages, this article proposes an *adaptive modular geometric control* framework for interconnected multi-body systems evolving on  $SE(3)$ . Building upon the subsystem-based principles of VDC, we reformulate the scheme entirely within a coordinate-free geometric setting, yielding a novel control architecture defined directly on the Lie group. The robotic system is decomposed into rigid-body and joint modules on  $SE(3)$ , and local control laws are synthesized while preserving closed-loop stability through geometric virtual power flow consistency. Furthermore, by combining a recursive product-of-exponentials representation with a recursive Newton–Euler formulation on  $SE(3)$ , the resulting implementation achieves linear computational complexity, scaling as  $\mathcal{O}(2n)$  with the number of bodies [9].

In particular, this work reformulates the VDC framework entirely within a differential-geometric setting, deriving a local geometric control law and a novel stability analysis directly on  $SE(3)$  rather than in Euclidean coordinates. Furthermore, parametric uncertainty is addressed through a geometric adaptive law evolving on  $\mathcal{P}(4)$ , requiring only a single global adaptation gain for the entire multi-body system while ensuring drift-free and physically consistent parameter estimation. The closed-loop system is shown to achieve exponential tracking stability without parametric uncertainties and semi-global uniformly ultimate boundedness in the presence of uncertainties, within the injectivity radius of the logarithmic map.

The remainder of the paper is organized as follows. Section II reviews the geometric preliminaries on  $SE(3)$  and the modular decomposition framework. Section III develops the modular geometric controller, and Section IV introduces the adaptive extension. Section V presents simulation results, followed by concluding remarks in Section VI.

## II. MATHEMATICAL PRELIMINARIES

### A. Notation and Geometric Preliminaries

*Definition 1 (Configuration Spaces and Matrix Manifolds):*

We denote by  $\mathbb{R}^n$  the  $n$ -dimensional Euclidean space with the standard inner product. The special orthogonal ( $SO(3)$ ) group and special Euclidean ( $SE(3)$ ) group are defined as,

$$SO(3) := \{R \in \mathbb{R}^{3 \times 3} \mid R^T R = I, \det(R) = 1\}, \quad (1)$$

$$SE(3) := \left\{ \mathcal{T} = \begin{bmatrix} R & p \\ 0 & 1 \end{bmatrix} \mid R \in SO(3), p \in \mathbb{R}^3 \right\}. \quad (2)$$

The Lie algebra of  $SE(3)$  is denoted by  $\mathfrak{se}(3)$  and is given by,

$$\mathfrak{se}(3) := \left\{ \hat{\xi} = \begin{bmatrix} \hat{\omega} & v \\ 0 & 0 \end{bmatrix} \mid \omega, v \in \mathbb{R}^3 \right\}, \quad (3)$$

Corresponding author: Mahdi Hejrati

All authors are with the Department of Engineering and Natural Science, Tampere University, 7320 Tampere, Finland (e-mail: mahdi.hejrati@tuni.fi, amirhossein.barjini@tuni.fi, gokhan.alcan@tuni.fi, jouni.mattila@tuni.fi).

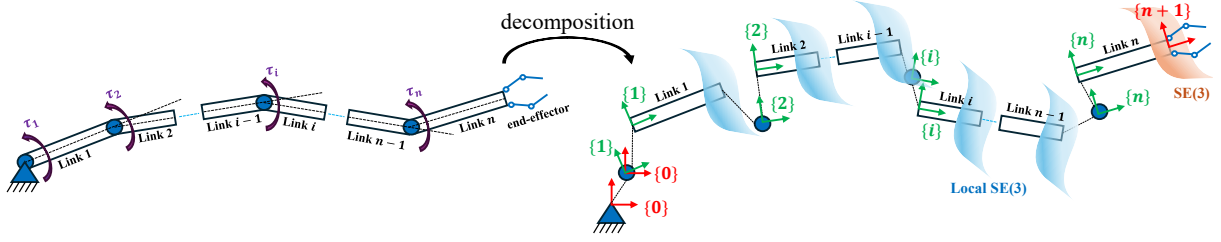


Fig. 1. Interconnected multi-rigid body system decomposed into modules of rigid body and joints.

where  $(\cdot)^\wedge : \mathbb{R}^6 \rightarrow \mathfrak{se}(3)$  is the standard skew-symmetric “hat” operator. The inverse map is denoted by  $(\cdot)^\vee$  so that  $\omega = \hat{\omega}^\vee$ . The Lie bracket of two elements  $\hat{V}_1 \in \mathfrak{se}(3)$  and  $\hat{V}_2 \in \mathfrak{se}(3)$  is defined as  $[\hat{V}_1, \hat{V}_2] = \hat{V}_1 \hat{V}_2 - \hat{V}_2 \hat{V}_1$ . The dual space of  $\mathfrak{se}(3)$ ,  $\mathfrak{se}^*(3)$ , is the space of the wrenches applied to a rigid body with the pair of  $(\tau, f)$ . The Lie group exponential map,  $\exp : \mathfrak{se}(3) \rightarrow SE(3)$ , provides a smooth mapping from the Lie algebra to the group, with local inverse given by the logarithm map,  $\log : SE(3) \rightarrow \mathfrak{se}(3)$ .

We use  $\mathcal{P}(4)$  to denote the manifold of symmetric positive definite  $4 \times 4$  matrices,

$$\mathcal{P}(4) := \{L \in \mathbb{R}^{4 \times 4} \mid L^\top = L, L \succ 0\}. \quad (4)$$

Since  $\mathcal{P}(4)$  is an open subset of the vector space of symmetric matrices, the tangent space at each  $L \in \mathcal{P}(4)$  can be identified with  $T_L \mathcal{P}(4) \cong \text{Sym}(4) := \{X \in \mathbb{R}^{4 \times 4} \mid X^\top = X\}$ .

*Definition 2 (Inner Products and Riemannian Metrics):*

The standard Euclidean inner product on  $\mathbb{R}^n$  is denoted by

$$\langle x, y \rangle := x^\top y, \quad x, y \in \mathbb{R}^n, \quad (5)$$

with associated norm  $\|x\| := \sqrt{\langle x, x \rangle}$ .

At the identity configuration  $\mathcal{T} = I \in SE(3)$  on the Lie algebra  $\mathfrak{se}(3)$ , the inner product

$$\langle \hat{V}_1, \hat{V}_2 \rangle_{(K, I)} := V_1^\top K V_2. \quad (6)$$

This inner product induces a left-invariant Riemannian metric on  $SE(3)$  [16].

On the manifold  $\mathcal{P}(4)$ , we use the affine-invariant Riemannian metric

$$\langle X, Y \rangle_L := \frac{1}{2} \text{tr}(L^{-1} X L^{-1} Y), \quad (7)$$

under group action of  $\mathcal{A} * L = \mathcal{A} L \mathcal{A}^\top$  with  $\mathcal{A} \in GL(4)$  being non-singular matrix with  $X, Y \in T_L \mathcal{P}(4)$ ,  $L \in \mathcal{P}(4)$  and induced norm  $\|X\|_L := \sqrt{\langle X, X \rangle_L}$ . When needed, we write  $\|\cdot\|_{\hat{L}_i}$  to emphasize that the norm is induced by the metric (7) at  $\hat{L}_i \in \mathcal{P}(4)$ .

## B. Manipulator Kinematics

For the  $n$ -DoF interconnected rigid bodies shown in Fig. 1,  $\mathcal{P} \in SE(3)$  and  $\mathcal{P}^d \in SE(3)$  represent the end-effector actual and desired pose. Such system can be decomposed into rigid body and joint subsystems, as shown in Fig. 1.

*Assumption 1:* There exists a mapping  $\mathcal{K}^d : \mathcal{P}^d \rightarrow \mathcal{T}^d$ , where  $\mathcal{T}^d = [\mathcal{T}_i^d] \in SE(3)$  for  $i = 1, \dots, n$ . Similarly, there

exists a mapping  $\mathcal{K} : \mathcal{P} \rightarrow \mathcal{T}$ , with  $\mathcal{T} = [\mathcal{T}_i] \in SE(3)$ . Accordingly,  $\mathcal{T}_i = (R_i, p_i)$  and  $\mathcal{T}_i^d = (R_i^d, p_i^d)$  denote the actual and desired local homogeneous transformation matrices of each body frame in the decomposed system.

We desire to derive the local homogeneous matrices with respect to the preceding bodies as,

$$\mathcal{T}_{i-1,i}(\theta_i) = \mathcal{T}_{i-1,i}(0) e^{\hat{\xi}_i \theta_i}, \quad (8)$$

where  $\hat{\xi}_i \in \mathfrak{se}(3)$  is the constant twist of the body frame and  $\mathcal{T}_{i-1,i}$  indicates the transformation matrix of frame  $\{i\}$  with respect to  $\{i-1\}$ , with  $\mathcal{T}_{i-1,i}(0)$  being the initial configuration between the frames. Additionally,  $\theta_i \in \mathbb{S}^n$  and  $\dot{\theta}_i \in T_{\theta} \mathbb{S}^4$  with  $\mathbb{S}^n = \mathbb{S}^1 \times \dots \times \mathbb{S}^1$  is the joint generalized coordinate. We can derive  $\mathcal{T}_i^d$  in the sense of (8) as,

$$\mathcal{T}_{i-1,i}^d(\theta_i^d) = \mathcal{T}_{i-1,i}(0) e^{\hat{\xi}_i \theta_i^d}. \quad (9)$$

In this formulation, the motion of the individual rigid bodies is preserved on  $SE(3)$  rather than being reduced to joint-space coordinates. The local transformation matrices expressed in the inertial frame can be written as  $\mathcal{T}_j = \prod_{i=1}^j \mathcal{T}_{i-1,i}(\theta_i)$ , where the product follows the recursive chain structure of the mechanism.

Let  $\mathcal{T}_i, \mathcal{T}_i^d \in SE(3)$  denote the actual and desired poses of rigid body  $i$ , then the local configuration error can be defined as,

$$e_i = (\mathcal{T}_i^d)^{-1} \mathcal{T}_i = \begin{bmatrix} (R_i^d)^T R_i & (R_i^d)^T (p_i - p_i^d) \\ 0 & 1 \end{bmatrix}. \quad (10)$$

The associated Lie-algebraic local configuration error is represented as,

$$\eta_i := \log(e_i)^\vee \in \mathbb{R}^6. \quad (11)$$

*Definition 3:* Given  $K_{z_i} \succ 0$ , the local configuration energy error of body  $i$  is defined in the sense of (6) as,

$$\Psi_i(e_i) = \frac{1}{2} \langle \log(e_i), \log(e_i) \rangle_{(K_{z_i}, I)} = \frac{1}{2} \eta_i^\top K_{z_i} \eta_i. \quad (12)$$

Since  $K_{z_i}$  is positive definite,  $\Psi_i$  is locally positive definite with respect to the identity  $e_i = I$  and provides a quadratic measure of configuration deviation within the injectivity domain of the logarithm map.

For each decomposed rigid body floating in space, we can write,

$$\dot{\mathcal{T}}_i = \mathcal{T}_i \hat{\mathcal{V}}_i. \quad (13)$$

with  $\hat{\mathcal{V}}_i = (\hat{w}_i, v_i) \in \mathfrak{se}(3)$  is the body-fixed velocity expressed in the body frame with respect to the spatial frame

and  $\dot{\mathcal{T}}_i \in T_{\mathcal{T}_i}SE(3)$  is the tangent vector of  $\mathcal{T}_i$ . In order to keep the modularity of the control framework through recursive approach, we extend (13) to,

$$\mathcal{V}_i = Ad_{\mathcal{T}_{i-1,i}^{-1}} \mathcal{V}_{i-1} + \mathcal{V}_{i-1,i}, \quad (14)$$

where by using  $\hat{\mathcal{V}}_{i-1,i} = \mathcal{T}_{i-1,i}^{-1} \dot{\mathcal{T}}_{i-1,i}$  and replacing from (8), one can establish,

$$\mathcal{V}_i = Ad_{\mathcal{T}_{i-1,i}^{-1}} \mathcal{V}_{i-1} + \xi_i \dot{\theta}_i, \quad (15)$$

where  $Ad_{\mathcal{T}}$  is the Adjoint map. As a result, (15) represents the body-fixed velocity of each local rigid bodies in terms of adjacent bodies. By taking the time-derivative of (15), one can establish the analytic representation of body-fixed acceleration,

$$\mathcal{A}_i = Ad_{\mathcal{T}_{i-1,i}^{-1}} \mathcal{A}_{i-1} + Ad_{\mathcal{T}_{i-1,i}^{-1}} [\xi_i \dot{\theta}_i, \mathcal{V}_{i-1}] + \xi_i \ddot{\theta}_i. \quad (16)$$

The desired terms  $\mathcal{V}_i^d$  and  $\mathcal{A}_i^d$  are computed by replacing  $\theta_i$  with  $\theta_i^d$  in (15) and (16), respectively.

### C. Manipulator Dynamics

Given the geometric representation of the modular system kinematics, the dynamics of each local subsystem can be expressed in terms of spatial wrenches. Consider a single decomposed rigid body in space. The net wrench acting on body  $i$  is given by,

$$\mathcal{F}_i = F_i - Ad_{\mathcal{T}_{i,i+1}^{-1}}^\top F_{i+1}, \quad (17)$$

where  $F_i \in \mathfrak{se}^*(3)$  and  $F_{i+1} \in \mathfrak{se}^*(3)$  denote the body-frame representations of the wrenches applied at the origins of frames  $\{i\}$  and  $\{i+1\}$ , respectively. On the other hand, the net wrench of rigid body  $i$  can be written using the Newton–Euler equation as,

$$\mathcal{F}_i = M_i \mathcal{A}_i - ad_{\mathcal{V}_i}^* (M_i \mathcal{V}_i), \quad (18)$$

where  $M_i \in \mathbb{R}^{6 \times 6}$  is the spatial inertia matrix,  $\mathcal{V}_i$  is the body twist,  $\mathcal{A}_i$  is the body acceleration, and  $ad_{\mathcal{V}_i}^*$  denotes the co-adjoint operator. Consequently, the recursive wrench relation becomes,

$$F_i = M_i \mathcal{A}_i - ad_{\mathcal{V}_i}^* (M_i \mathcal{V}_i) + Ad_{\mathcal{T}_{i,i+1}^{-1}}^\top F_{i+1}. \quad (19)$$

### D. Virtual Stability

So far, the modular geometric representation of the kinematics and dynamics has been derived for the decomposed interconnected multi-body system, consistent with the formulations in [17]–[19]. To enforce the physical constraints of the connected system, we adopt the concept of virtual power flow (VPF) introduced in [9]. The VPF is a virtual power term defined for each rigid body that captures its dynamic interaction with neighboring bodies. For two adjacent subsystems, the VPF acting on the  $i$ th body has equal magnitude and opposite sign to that acting on the  $(i+1)$ th body. Consequently, when the subsystem dynamics are composed, the VPF terms cancel, thereby enforcing the interconnection constraints of the original multi-body system.

Let  $\mathcal{V}_i^r$ , to be defined subsequently, denote the *required* body velocity, and let  $F_i^r$  represent the *required* wrench for the  $i$ th rigid body. The term *required* refers to the value that the corresponding quantity in the rigid-body dynamics must attain in order to achieve the prescribed behavior. Based on this notion, the VPF between the  $i$ th rigid body and its adjacent subsystem is defined as [9]

$$p_i = (\mathcal{V}_i^r - \mathcal{V}_i)^\top (F_i^r - F_i), \quad (20)$$

which measures the virtual power mismatch resulting from deviations between the required and actual velocities and wrenches. Geometrically, this expression corresponds to the natural dual pairing between the Lie algebra  $\mathfrak{se}(3)$  (body velocity) and its dual space  $\mathfrak{se}^*(3)$  (wrench). It may therefore be interpreted as a virtual constraint interaction that encodes the compatibility condition between adjacent subsystems. In a properly composed modular system, the VPFs of neighboring subsystems cancel (i.e.,  $p_i = -p_{i+1}$ ), thereby enforcing dynamic consistency and enabling distributed stability analysis.

*Definition 4:* Let  $V_i : \mathbb{R}^n \rightarrow \mathbb{R}_{\geq 0}$  be a continuously differentiable function satisfying

$$\underline{\alpha}_i \|x_i\|^2 \leq V_i(x_i) \leq \bar{\alpha}_i \|x_i\|^2, \quad (21)$$

for all  $x_i \in \mathbb{R}^n$  of subsystem  $i$  with  $\underline{\alpha}, \bar{\alpha} > 0$ . Suppose that along the trajectories of the  $i$ -th subsystem, the time derivative of  $V_i$  satisfies

$$\dot{V}_i(x_i, t) \leq -\tilde{\alpha}_i \|x_i\|^2 + p_i - p_{i+1} + \bar{\epsilon}_i, \quad (22)$$

with  $\tilde{\alpha}_i > 0$ ,  $\bar{\epsilon}$  being unknown positive constant, and  $p_i \in \mathbb{R}$  denotes the virtual power flow between adjacent subsystems. Then, the  $i$ -th subsystem is virtually stable [9], [12].

As indicated by Definition 4, in the absence of VPFs, the time derivative of  $V_i$  satisfies the exponential stability condition when  $\bar{\epsilon}_i = 0$ , i.e., in the absence of parametric uncertainty, and semi-global uniform ultimate boundedness in the presence of uncertainties.

## III. MODULAR GEOMETRIC CONTROL

In this section we will elaborate on the design of modular geometric control method for an interconnected rigid body system in absence of uncertainty. Instead of designing the geometric control in the end-effector space, we break the desired behavior of the end-effector  $\mathcal{P}^d$  to the desired local homogeneous matrix of each rigid body  $\mathcal{T}_{i-1,i}^d$  after which the local modular geometric control can be designed.

The local configuration error  $\eta_i$  is defined in (11). However, defining the body velocity error in geometric approach is not as trivial. From (13) we can see that  $\dot{\mathcal{T}}_i \in T_{\mathcal{T}_i}SE(3)$  while  $\dot{\mathcal{T}}_i^d \in T_{\mathcal{T}_i^d}SE(3)$ , which shows that actual and desired tangent vectors do not belong to the same tangent space. This implies that to compute the velocity error we cannot just simply compare them as if they belong to the same space. In contrast, we will define the body velocity error as,

$$\mathcal{V}_i^e = Ad_{e^{-1}} \mathcal{V}_i^d - \mathcal{V}_i. \quad (23)$$

where  $Ad_{e_i^{-1}}$  maps the desired velocity to the space where the  $\mathcal{V}_i$  resides. Now, the required body velocity  $\mathcal{V}_i^r \in R^6$  can be defined as,

$$\mathcal{V}_i^r = Ad_{e_i^{-1}} \mathcal{V}_i^d - \Gamma_i \eta_i, \quad (24)$$

with  $\Gamma_i$  being positive definite gain. Defining the required body-fixed velocity as a logarithmic function of local natural error allows for more smoother convergence to the origin [1]. The definition of  $\mathcal{V}_i^r$  in the sense of (24) enables the geometric motion of each single rigid bodies on the manifold instead of just considering the end-effector. The required body acceleration, on the other hand, can be computed by taking the time derivative of (24) as,

$$\mathcal{A}_i^r = Ad_{e_i^{-1}} \mathcal{A}_i^d + Ad_{e_i^{-1}} [V_{e_i}, \mathcal{V}_i^d] - \Gamma_i \mathcal{B}_X \mathcal{V}_i^e, \quad (25)$$

with,

$$\mathcal{B}_X = \sum_0^{\infty} \frac{(-1)^n B_n}{n!} ad_{\eta_i}^n, \quad (26)$$

where  $B_n$  is the Bernoulli numbers. Now the required wrench of the  $i^{th}$  body can be expressed by replacing  $\mathcal{V}_i$  and  $\mathcal{A}_i$  in (19) with  $\mathcal{V}_i^r$  and  $\mathcal{A}_i^r$ , respectively,

$$F_i^r = M_i \mathcal{A}_i^r - ad_{\mathcal{V}_i^r}^* (M_i \mathcal{V}_i^r) + K_v (\mathcal{V}_i^r - \mathcal{V}_i) + Ad_{T_{i,i+1}^T} F_{i+1}^r. \quad (27)$$

The last term in (27) propagates the required wrench from the successive bodies. Finally, the control input applied at the joints is computed as,

$$\tau_i^r = \xi_i^\top F_i^r + \mathcal{J}_i^r, \quad (28)$$

where  $\mathcal{J}_i^r$  denotes the contribution arising from the joint dynamics. The required torque in (28) results from the composition of the decomposed rigid-body and joint subsystems. The first term on the right-hand side accounts for the rigid-body motion on SE(3), where the screw axis  $\xi_i$  enforces the joint constraint and maps the required wrench to the corresponding joint torque. The second term represents the contribution of the joint dynamics. A critical component in composing the required joint action is the required joint velocity  $\dot{\theta}_i^r$ , analogous to the required body velocity defined in (24). To derive this term, assume an electric actuator driving the  $i$ th joint with the following dynamics,

$$I_{m_i} \ddot{\theta}_i = \mathcal{J}_i, \quad (29)$$

where  $\mathcal{J}_i$  denotes the net torque applied to the joint. The net torque is given by,

$$\mathcal{J}_i = \tau_i - \xi_i^\top F_i, \quad (30)$$

with  $\tau_i$  being the actuator torque and  $\xi_i^\top F_i$  representing the torque induced by the rigid-body wrench. The required joint action is, then, defined as,

$$\mathcal{J}_i^r = I_{m_i} \ddot{\theta}_i^r + k_{ai} (\dot{\theta}_i^r - \dot{\theta}_i), \quad (31)$$

where  $k_{ai} > 0$  is a control gain. The required joint velocity satisfies,

$$\xi_i \dot{\theta}_i^r = \mathcal{V}_i^r - Ad_{T_{i-1,i}^{-1}} \mathcal{V}_{i-1}^r, \quad (32)$$

which enforces kinematic consistency between adjacent sub-systems.

*Theorem 1:* Consider a complex robotic system which is decomposed into the subsystems, as shown in Fig. 1, with the rigid body and joint dynamics of (19) and (29), respectively. Each subsystem is virtually stable in the sense of Definition 4 under the modular geometric control (27) and (31).

*Proof:* We start the proof by considering the rigid-body subsystem. Let us define the Lyapunov function as,

$$V_i = \frac{1}{2} (\mathcal{V}_i^r - \mathcal{V}_i)^T M_i (\mathcal{V}_i^r - \mathcal{V}_i) + \Psi_i(e_i). \quad (33)$$

with  $\Psi_i(e_i)$  defined in Definition 3. Subtracting (19) from (27), we have,

$$F_i^r - F_i = M_i (\mathcal{A}_i^r - \mathcal{A}_i) - ad_{\mathcal{V}_i^r}^* M_i (\mathcal{V}_i^r - \mathcal{V}_i) + K_v (\mathcal{V}_i^r - \mathcal{V}_i) + Ad_{T_{i,i+1}^T} (F_{i+1}^r - F_{i+1}). \quad (34)$$

Now, by taking the time derivative of (33) and replacing from (34), we have,

$$\begin{aligned} \dot{V}_i &= (\mathcal{V}_i^r - \mathcal{V}_i)^T (F_i^r - F_i) - (\mathcal{V}_i^r - \mathcal{V}_i)^T K_v (\mathcal{V}_i^r - \mathcal{V}_i) \\ &\quad - (\mathcal{V}_i^r - \mathcal{V}_i)^T Ad_{T_{i,i+1}^T} (F_{i+1}^r - F_{i+1}) \\ &\quad + (\mathcal{V}_i^r - \mathcal{V}_i)^T ad_{\mathcal{V}_i^r}^* M_i (\mathcal{V}_i^r - \mathcal{V}_i) - \eta_i^T K_{z_i} \mathcal{V}_i^e \\ &= p_i - p_{i+1} - (\mathcal{V}_i^r - \mathcal{V}_i)^T K_v (\mathcal{V}_i^r - \mathcal{V}_i) \\ &\quad - \eta_i^T K_{z_i} \mathcal{V}_i^e + (\mathcal{V}_i^r - \mathcal{V}_i)^T ad_{\mathcal{V}_i^r}^* M_i (\mathcal{V}_i^r - \mathcal{V}_i). \end{aligned} \quad (35)$$

In (35), the matrix  $ad_{\mathcal{V}_i^r}^* M_i$  is not inherently skew-symmetric. To address this issue, we employ Young's inequality together with the upper bound assumption for  $\|ad_{\mathcal{V}_i^r}^* M_i\| \leq \mathcal{C}_i \|\mathcal{V}_i\|$  where  $\mathcal{C}_i > 0$  is a constant depending on the inertia matrix. Accordingly, one can obtain,

$$\begin{aligned} &(\mathcal{V}_i^r - \mathcal{V}_i)^T ad_{\mathcal{V}_i^r}^* M_i (\mathcal{V}_i^r - \mathcal{V}_i) \\ &\leq (\mathcal{V}_i^r - \mathcal{V}_i)^T \left( \frac{1}{2\alpha_i} + 2\alpha_i \mathcal{C}_i^2 \right) (\mathcal{V}_i^r - \mathcal{V}_i) \end{aligned} \quad (36)$$

with  $\sup_{t>0} \|\mathcal{V}_i\| = \hat{\mathcal{C}}_i < \infty$  and  $\bar{\mathcal{C}}_i = \mathcal{C}_i \hat{\mathcal{C}}_i$ . Then, replacing above in (35) yields to,

$$\begin{aligned} \dot{V}_i &\leq -\frac{1}{2} (\mathcal{V}_i^r - \mathcal{V}_i)^T \mu_i (\mathcal{V}_i^r - \mathcal{V}_i) - \eta_i^T K_{z_i} \mathcal{V}_i^e \\ &\quad + p_i - p_{i+1}. \end{aligned} \quad (37)$$

which, by using  $\mathcal{V}_i^r - \mathcal{V}_i = \mathcal{V}_i^e - \Gamma_i \eta_i$  through (23) and (24), exploiting left-invariance property of (6) [16, Theorem 1] along with employing Cauchy-Schwarz and Young's inequalities and  $\rho_i = \max(\lambda_{max}(M_i), \lambda_{max}(K_{z_i}))$ , with  $\lambda_{max}(\cdot)$  being maximum eigenvalue, one can obtain,

$$\dot{V}_i \leq -\rho_i V_i + p_i - p_{i+1}, \quad (38)$$

with  $\rho_i = \min(\mu_i, 2\bar{\mu}_i)/\rho_i/8$ ,  $\mu_i = 2K_v - \frac{1}{\alpha_i} + \alpha_i \mathcal{C}_i^2 > 0$ ,  $\bar{K}_{z_i} = \Gamma_i \mu_i - K_{z_i} > 0$ ,  $\bar{\mu}_i = \Gamma_i \mu_i \Gamma_i - 2\epsilon^{-1} \bar{K}_{z_i} > 0$ , and  $2\epsilon_i \leq \mu_i \bar{K}_{z_i}^{-1}$ . It follows from (38) that the virtual exponential stability of the rigid body subsystem is achieved.

In order to investigate the stability of the joint subsystems, we define,

$$V_{ai} = \frac{1}{2} I_{m_i} (\dot{\theta}_i^r - \dot{\theta}_i)^2, \quad (39)$$

and by subtracting (29) from (31) and replacing in the time derivative of (39), we have,

$$\dot{V}_{ai} = (\dot{\theta}_i^r - \dot{\theta}_i) (\mathcal{J}_i^r - \mathcal{J}_i) - k_{ai}(\dot{\theta}_i^r - \dot{\theta}_i)^2. \quad (40)$$

Now, by using (28) and (30), we have,

$$\dot{V}_{ai} = (\dot{\theta}_i^r - \dot{\theta}_i) \xi_i^T (F_i^r - F_i) - k_{ai}(\dot{\theta}_i^r - \dot{\theta}_i)^2, \quad (41)$$

where we assumed  $\tau_i = \tau_i^r$  which is a reasonable assumption in the torque-controlled mode for the driver of the actuator. Now, we can extend (41) by using (32) and (15) as,

$$\begin{aligned} \dot{V}_{ai} &= -(\mathcal{V}_i^r - \mathcal{V}_i)^T (F_i^r - F_i) - k_{ai}(\dot{\theta}_i^r - \dot{\theta}_i)^2 \\ &\quad - Ad_{\mathcal{T}_{i-1,i}^{-1}} (\mathcal{V}_{i-1}^r - \mathcal{V}_{i-1}^r)^T (F_i^r - F_i) \\ &= -p_i + p_{i-1} - \frac{2k_{ai}}{I_{mi}} V_{ai}, \end{aligned} \quad (42)$$

demonstrating the virtual exponential stability of subsystem. ■

*Theorem 2:* The system of inter-connected rigid bodies decomposed into subsystems of rigid body and joint modules with the governing dynamics of (19) and (29) under the control action of (27) and (31) is exponentially stable.

*Proof:* We define the Lyapunov function of the unified system as,

$$V = \sum_{i=1}^n (V_i + V_{ai}), \quad (43)$$

which by taking its time derivative and replacing from Theorem 1 and the fact that  $\sum_{i=1}^n -p_i + p_{i-1} + p_i - p_{i+1} = p_0 - p_{n+1} = 0$  with the assumption of fixed ground for the base and no interaction with environment for the last frame, we have,

$$\dot{V} \leq -\underline{\varrho}V, \quad (44)$$

with  $\underline{\varrho} = \min_{i=1 \dots n} (\varrho_i, 2k_{ai}/I_{mi})$ . Consequently, one can show the exponential convergence of  $V \leq e^{-\underline{\varrho}t}V(0) \leq e^{-\underline{\varrho}t}\bar{\varrho}\|x(0)\|^2$  with  $\bar{\varrho} = \max(\rho_i, I_{mi})$ , which following from (44), (43), (33), and (12) leads to  $\|\Psi(e_i)\| \leq e^{-\underline{\varrho}t}\bar{\varrho}\|x(0)\|^2$ , demonstrating the non-singularity of the logarithmic map with the proper initialization. Moreover,  $x_i = [\dot{\theta}_i^r - \dot{\theta}_i, (\mathcal{V}_i^r - \mathcal{V}_i)^T, \eta_i^T]_{i=1}^n$ .

Now, we will show that our assumption regarding upper bound of the velocity,  $\sup_{t>0} \|\mathcal{V}_i\| = \hat{\mathcal{C}}_i$  is correct. From (44), it can be shown that  $\sup_{t>0} \|\mathcal{V}_i^r - \mathcal{V}_i\| \leq \sqrt{2\bar{\varrho}/\lambda_{\min}(M_i)}\|x(0)\|$ . Then, we can write by exploiting (23) and (24),

$$\sup_{t>0} \|\mathcal{V}_i\| \leq \sup_{t>0} \|\mathcal{V}_i^r - \mathcal{V}_i\| + \sup_{t>0} \|Ad_{e_i^{-1}} \mathcal{V}_i^d\| + \sup_{t>0} \|\Gamma_i \eta_i\|. \quad (45)$$

The inequality in (45) can be written in the following form by exploiting the first-order approximation of  $Ad_{e_i^{-1}} \leq 1 + \|\eta_i\|$ , boundedness of the desired velocity  $\|\mathcal{V}_i^d\| \leq N_i^d$ , we have,

$$\begin{aligned} \sup_{t>0} \|\mathcal{V}_i\| &\leq \left( \sqrt{\frac{2\bar{\varrho}}{\lambda_{\min}(M_i)}} (1 + N_i^d) \right. \\ &\quad \left. + \sqrt{\frac{2\lambda_{\max}(\Gamma_i)^2}{\lambda_{\min}(K_{z_i})}} \right) \|x(0)\|. \end{aligned} \quad (46)$$

#### IV. ADAPTIVE MODULAR GEOMETRIC CONTROL

While the modular structure has been established, parametric uncertainty in the rigid-body dynamics has not yet been addressed and may degrade performance. This section therefore develops an adaptive modular geometric control scheme to compensate for such uncertainties. Without loss of generality, the joint subsystems are assumed to retain the same control law as in the preceding section, and the adaptive design is therefore presented for the rigid-body modules.

Consider the equation of motion for a decomposed rigid body in space as in (19). In order to tackle the parameter uncertainty in inertial matrix, we need to develop an adaptive control law as,

$$F_i^r = \hat{M}_i \mathcal{A}_i^r - ad_{\mathcal{V}_i}^* (\hat{M}_i \mathcal{V}_i^r) + K_v (\mathcal{V}_i^r - \mathcal{V}_i) - Ad_{\mathcal{T}_{i,i+1}^{-1}} F_{i+1}^r. \quad (47)$$

This form of control action requires only update of spatial inertial matrix to tackle the parameter uncertainties in contrast to other methods that requires update of Centrifugal and gravitational matrices. In the following, a geometric adaptation law is designed that directly updates the spatial inertia matrix.

Consider  $L_i \in \mathcal{P}(4)$  and  $\hat{L}_i \in \mathcal{P}(4)$  being points on the manifold. The distance between two points  $L_i$  and  $\hat{L}_i$  on the manifold can be determined by the Bregman divergence as the pseudo-metric. For this aim, let  $h : \mathcal{P}(4) \rightarrow \mathbb{R}$  be  $\mathcal{C}^2$  and strictly convex function, the Bregman divergence of which can be computed as,

$$d_h(L_i || \hat{L}_i) = h(L_i) - h(\hat{L}_i) - \nabla h(L_i)^T (\hat{L}_i - L_i), \quad (48)$$

with the following properties: 1)  $d_h(\hat{L}_i || L_i) \geq 0$  with  $d_h(\hat{L}_i || L_i) = 0$  if  $\hat{L}_i = L_i$ , 2)  $d_h(\hat{L}_i || L_i)$  is strictly convex [20]. Considering  $h(L_i) = -\log|L_i|$ , the divergence metric in (49) is a second-order approximation of affine-invariant Riemannian metric (7). Consequently, the Bregman divergence metric in (49) with log-determinant function,

$$d_h(L_i || \hat{L}_i) = \gamma \left( \log \frac{|\hat{L}_i|}{|L_i|} + \text{tr}(\hat{L}_i^{-1} L_i) - 4 \right), \quad (49)$$

or

$$d_h(L_i || \hat{L}_i) = \sum_{j=1}^4 (-\log(\lambda_j) + \lambda_j - 1), \quad (50)$$

with  $\{\lambda_j\}_{j=1}^4$  are the eigenvalues of  $\hat{L}_i^{-1} L_i$ , is a valid Lyapunov function with its time derivative as,

$$\dot{d}_h(L_i || \hat{L}_i) = \gamma \left( \text{tr}((\hat{L}_i^{-1} \dot{\hat{L}}_i \hat{L}_i^{-1}) \tilde{L}_i) \right). \quad (51)$$

In the following, we will show that the update of pseudo-inertial matrix as,

$$\dot{\hat{L}}_i = \frac{1}{\gamma} \hat{L}_i \hat{\mathcal{L}}_i \hat{L}_i - \sigma(\hat{L}_i - L_i^0) \quad (52)$$

with  $L_i^0 \succ 0$  being nominal value for the estimation, will keep the geometric property of the controller and adaptation consistent, yet requiring only one adaptation gain  $\gamma$  for the entire inter-connected rigid body system along with ensuring the physical consistency of the estimated inertial parameters. ■

As stated in [7], there is a one-to-one mapping between  $L_i$  and  $M_i$  as follow:

$$\begin{aligned} L_i &= f(M_i) = f(I_{A_i}, h_{A_i}, m_i) = \begin{bmatrix} \Sigma_{A_i} & h_{A_i} \\ h_{A_i}^T & m_i \end{bmatrix}, \\ M_i &= f^{-1}(\Sigma_{A_i}, h_{A_i}, m_i) = \begin{bmatrix} I_{A_i} & h_{A_i} \\ -h_{A_i} & m_i I_i \end{bmatrix} \end{aligned} \quad (53)$$

with  $\Sigma_{A_i} = \text{trace}(I_{A_i}) - I_{A_i}$ .

*Lemma 1:* For the Bregman divergence defined in (49), the following upper bound for some constant  $C_i > 0$  holds,

$$d_h(L_i \| \hat{L}_i) \leq C_i \left( \|E_i\|_{\hat{L}_i}^2 + \|L_i - L_i^0\|_{\hat{L}_i}^2 \right). \quad (54)$$

*Proof:* First, define the parameter estimation error and auxiliary variable as,

$$\tilde{L}_i := \hat{L}_i - L_i \in \text{Sym}(4), \quad E_i := \hat{L}_i - L_i^0 \in \text{Sym}(4), \quad (55)$$

from which,

$$\tilde{L}_i = E_i - (L_i - L_i^0). \quad (56)$$

Let us define the geodesic distance derived from metric (7) as,

$$d_R(L, \hat{L}) := \left\| \log(L^{-\frac{1}{2}} \hat{L} L^{-\frac{1}{2}}) \right\|, \quad (57)$$

or

$$d_R(L, \hat{L}) = \left( \sum_{j=1}^4 (\log \bar{\lambda}_j)^2 \right)^{\frac{1}{2}}. \quad (58)$$

with  $\{\bar{\lambda}_j\}_{j=1}^4$  being the eigenvalues of  $L^{-1} \hat{L}$  with  $\lambda_j = \bar{\lambda}_j^{-1}$ . Now, for any compact set  $\mathcal{K} \subset \mathcal{P}(4)$ , by Taylor's approximation theorem applied to (50) and (58), there exists a constant  $c > 0$  such that

$$d_h(L \| \hat{L}) \leq c d_R(L, \hat{L})^2, \quad \forall L, \hat{L} \in \mathcal{K}, \quad (59)$$

where,

$$c = \frac{1}{2} e^\delta, \quad \delta := \sup_{L, \hat{L} \in \mathcal{K}} \lambda_{\max}(|\log(L^{-1} \hat{L})|).$$

Considering the square of triangle inequality for the distance metric (57) according to Fig. 2 and using  $(a+b)^2 \leq 2(a^2 + b^2)$ , the following upper bound can be established,

$$d_h(L_i \| \hat{L}_i) \leq 2c \left( d_R(L_i, L_i^0)^2 + d_R(L_i^0, \hat{L}_i)^2 \right). \quad (60)$$

Moreover, the affine-invariant distance (57) is Lipschitz equivalent to the ambient norm on  $\mathcal{K}$ . Hence, there exist constants  $k_{C,i}, k_{E,i} > 0$  such that, for all  $L_i, L_i^0, \hat{L}_i \in \mathcal{K}$ ,

$$\begin{aligned} d_R(L_i, L_i^0)^2 &\leq k_{C,i} \|L_i - L_i^0\|_{\hat{L}_i}^2, \\ d_R(L_i^0, \hat{L}_i)^2 &\leq k_{E,i} \|\hat{L}_i - L_i^0\|_{\hat{L}_i}^2, \end{aligned} \quad (61)$$

Finally, substituting (61) into (60) will yield to (54) with  $C_i := 2c \max\{k_{C,i}, k_{E,i}\}$ . ■

To facilitate the subsequent stability analysis, the adaptive modular geometric control law in (47) is rewritten in the following equivalent form,

$$\begin{aligned} (\mathcal{V}_i^r - \mathcal{V}_i)^T (\hat{M}_i \mathcal{A}_i^r - \text{ad}_{\mathcal{V}_i}^* (\hat{M}_i \mathcal{V}_i^r)) &= \text{tr}(\hat{L}_i \hat{\mathcal{L}}_i), \\ (\mathcal{V}_i^r - \mathcal{V}_i)^T (M_i \mathcal{A}_i - \text{ad}_{\mathcal{V}_i}^* (M_i \mathcal{V}_i)) &= \text{tr}(L_i \mathcal{L}_i) \end{aligned} \quad (62)$$

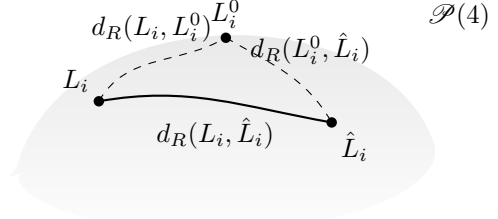


Fig. 2. Geometric illustration of the SPD manifold  $\mathcal{P}(4)$  with the true inertia  $L_i$ , estimate  $\hat{L}_i$ , and nominal model  $L_i^0$ . The curves indicates the Riemannian geodesic between the points on the manifold.

where  $\mathcal{L}_i$  is a unique symmetric matrix, defined in [20]. On the other hand, by subtracting (19) from (47) along with adding  $(\mathcal{V}_i^r - \mathcal{V}_i)^{-T} (\text{tr}(L_i \mathcal{L}_i) - \text{tr}(L_i \hat{\mathcal{L}}_i))$  and using (62), we have,

$$\begin{aligned} M_i (\mathcal{A}_i^r - \mathcal{A}_i) &= (F_i^r - F_i) - (\mathcal{V}_i^r - \mathcal{V}_i)^{-T} \text{tr}(\tilde{L}_i \hat{\mathcal{L}}_i) \\ &\quad + \text{Ad}_{\mathcal{V}_i^r}^T (F_{i+1}^r - F_{i+1}) \\ &\quad + \text{ad}_{\mathcal{V}_i}^* (M_i (\mathcal{V}_i^r - \mathcal{V}_i)) - K_v (\mathcal{V}_i^r - \mathcal{V}_i). \end{aligned} \quad (63)$$

*Theorem 3:* Consider a complex robotic system decomposed into the subsystems, as shown in Fig. 1, with the rigid body and joint dynamics of (19) and (29) in the presence of parameter uncertainties. Each subsystem is virtually stable in the sense of Definition 4 under the adaptive modular geometric control (47) and (31) and adaptation law (52).

*Proof:* Define the local Lyapunov function as,

$$v_i = V_i + d_h(L_i \| \hat{L}_i). \quad (64)$$

First we investigate the time derivative of  $d_h(L_i \| \hat{L}_i)$  in (51). By substituting (52) in (51) and using (56), we have,

$$\dot{d}_h = \text{tr}(\hat{\mathcal{L}}_i \tilde{L}_i) - \gamma \sigma \text{tr}(\hat{L}_i^{-1} E_i \hat{L}_i^{-1} \tilde{L}_i), \quad (65)$$

with the second term,

$$\text{tr}(\hat{L}_i^{-1} E_i \hat{L}_i^{-1} \tilde{L}_i) = 2 \langle E_i, \tilde{L}_i \rangle_{\hat{L}_i}. \quad (66)$$

Substituting (56) into (66) in the sense of (7), we have,

$$\langle E_i, \tilde{L}_i \rangle_{\hat{L}_i} = \|E_i\|_{\hat{L}_i}^2 - \langle E_i, L_i - L_i^0 \rangle_{\hat{L}_i}. \quad (67)$$

Now, by applying Young's inequality to the second term of (67) for any  $\beta_i > 0$  and substituting all in (65) yields,

$$\dot{d}_h \leq \text{tr}(\hat{\mathcal{L}}_i \tilde{L}_i) - \gamma \sigma (1 - \beta_i) \|E_i\|_{\hat{L}_i}^2 + \frac{\gamma \sigma}{4\beta_i} \|L_i - L_i^0\|_{\hat{L}_i}^2. \quad (68)$$

Now, by replacing (68) in the time derivative of (64) and using (63), (43), and (54) along with following the same procedure in (35) and (36), we have,

$$\dot{v}_i \leq -\Omega_i v_i + \varepsilon_i \quad (69)$$

with  $\Omega_i = \min(\varrho_i, \varpi_i C_i^{-1}) / \bar{\rho}_i$ ,  $\bar{\rho} = \max(\rho_i, 1)$ ,  $\varepsilon_i = 2_i \varpi_i \|L_i - L_i^0\|_{\hat{L}_i}^2$ ,  $\varpi_i = \gamma \sigma_i \min((1 - \beta_i), 1/(4\beta_i))$ . Now, by considering the procedure for the joint subsystems as in (39)-(42), defining the total Lyapunov function as  $v_T =$

$\sum_1^n (V_{ai} + v_i)$ , taking its time derivative and replacing from (69), one can obtain,

$$\dot{v}_T \leq -v v_T + \varepsilon, \quad (70)$$

with  $v = \min(\Omega_i, 2k_{ai}/I_{mi})$  and  $\varepsilon = \min(\varepsilon_i)$ . Then, the following can be obtained,

$$v_T(t) \leq v_T(0)e^{-vt} + \frac{\varepsilon}{v}(1 - e^{-vt}) \leq v_T(0) + \frac{\varepsilon}{v}, \quad (71)$$

Therefore, all closed-loop trajectories remain bounded for all  $t \geq 0$ , and the origin of the error dynamics is semi-globally uniformly ultimately bounded with respect to an ultimate bound proportional to  $\varepsilon/v$ . Additionally, by defining the following according to (50),

$$\phi(\lambda) := -\log \lambda + \lambda - 1, \quad \lambda > 0, \quad (72)$$

the following can be shown as a result of (71) and (64),

$$\lambda_{\max}(\hat{L}_i^{-1}L_i) \leq \bar{\lambda} = \phi^{-1}(v_T(0) + \frac{\varepsilon}{v}), \quad (73)$$

demonstrating the boundedness of the parameter estimation error on the manifold. Furthermore, following the same procedure in the last section, the upper bound for the  $\sup_{t>0} \|\mathcal{Y}_i\|$  can be obtained. It must be noted that by proper initialization that satisfies  $v_T(0) \leq -\frac{\varepsilon}{v} + \lambda_{\min}(K_{z_i})\pi^2/2$ , the local configurational error  $\eta_i$  will remain in non-singular region with  $\text{trace}(R_{e_i}) \geq -1$ . ■

## V. RESULTS

In this section, numerical simulations of a 4R redundant heavy-duty manipulator (total mass  $\approx 9350$  kg, reach  $\approx 7$  m) are conducted to evaluate the proposed controller. The system is modeled in MATLAB/Simulink with a sampling frequency of 1 kHz. The proposed modular geometric controller (MGC) and its adaptive extension (AMGC) are compared with the modular controller in [11] (VDC) and the geometric impedance controller in [3] (GIC). Due to a non-disclosure agreement (NDA) with the industrial partner, the detailed physical parameters of the manipulator cannot be publicly disclosed. All simulations are nevertheless performed using the actual system parameters to ensure faithful representation of the real platform.

Two scenarios are considered to investigate the convergence properties of the closed-loop system: (i) non-adaptive control without parametric uncertainty, with comparison against VDC and GIC; and (ii) adaptive control under a 10% perturbation of the inertial parameters. The controller gains are chosen as  $\Gamma_1 = 5\mathbb{I}_6$ ,  $\Gamma_{2,3} = 3\mathbb{I}_6$ ,  $\Gamma_4 = 1.5\mathbb{I}_6$ ,  $K_v = 2000\mathbb{I}_6$ ,  $k_{a1} = 10000$ ,  $k_{a2} = 20000$ ,  $k_{a3} = 10000$ ,  $k_{a4} = 350$ ,  $\gamma = 8 \times 10^4$ , where  $\mathbb{I}_N$  denotes as the  $N \times N$  identity matrix. For the VDC method [11], the gains are set to  $\Gamma = 5\mathbb{I}_6$ , while adopting the same  $K_v$  and  $K_{ai}$  values as those used in the proposed controller. For the GIC in equation (32) of [3] the tuned gains are  $K_P = 2500\mathbb{I}_3$ ,  $K_R = 25000\mathbb{I}_3$ ,  $K_V = 8000\mathbb{I}_4$ .

Figs. 3(a)–(c) show the convergence of the set-point reaching errors to the origin in the  $xy$ ,  $yz$ , and  $xz$  planes,

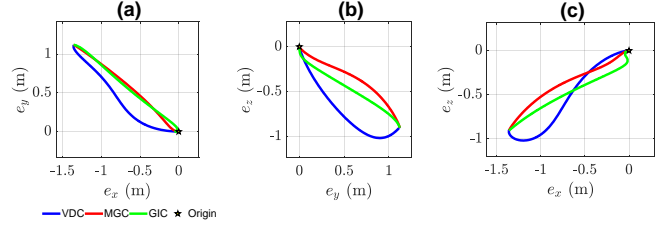


Fig. 3. Simulation comparison of the different controllers based on position tracking performance. Error convergence in (a) x-y plane, (b) y-z plane, and (c) x-z plane.

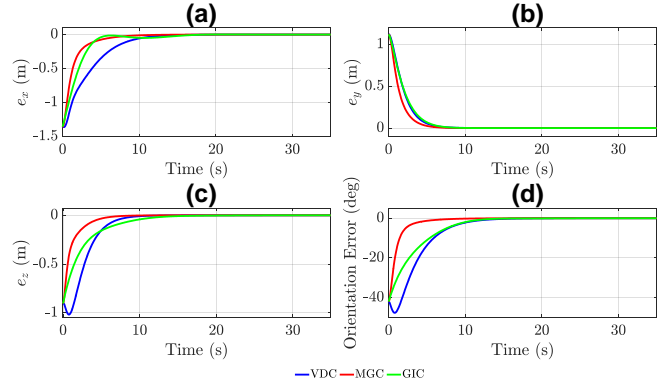


Fig. 4. Time history of the error convergence. Position error in (a) x direction, (b) y direction, (c) z direction, and (d) orientation error.

respectively. Additionally, Fig. 4 depicts the time history of the position and orientation errors, with Figs. 4(a)–(c) and Fig. 4(d) corresponding to position and orientation, respectively. As can be observed, both geometric controllers (GIC and the proposed MGC) achieve faster and smoother convergence compared to VDC. Moreover, the proposed MGC exhibits faster convergence than GIC, which can be attributed to the use of the logarithm of the natural error in the feedback law.

Fig. 5 presents the position error convergence of AMGC and MGC in the presence of parametric uncertainty. As can be seen, MGC exhibits a noticeable steady-state offset, whereas the AMGC is able to compensate for the uncertainties and drive the error closer to the origin. The corresponding time history of the error convergences are illustrated in Fig. 6, showing the enhanced performance for the convergence under AMGC. Finally, Fig. 7 depicts the time histories of the norms of the parameter estimation, confirming their boundedness and convergence, in accordance with the theoretical analysis.

## VI. CONCLUSION

This paper proposed an adaptive modular geometric control framework for interconnected rigid-body systems evolving on  $SE(3)$ . By decomposing the dynamics into rigid-body and joint subsystems and enforcing VPF constraints, the resulting controller preserves the geometric structure of the motion while enabling a recursive Newton–Euler implementation with computational complexity of order  $O(2n)$ . A geometric, drift-free adaptive law on the manifold of

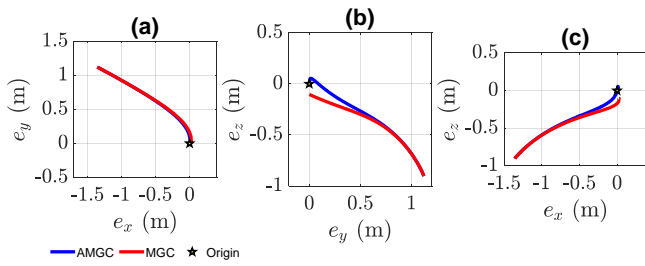


Fig. 5. Comparison of AMGC and MGC under parametric uncertainties. Error convergence in (a) x-y plane, (b) y-z plane, and (c) x-z plane.

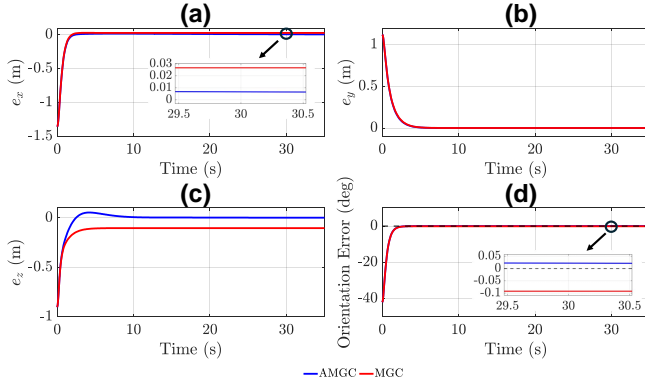


Fig. 6. Time history of the error convergence. Position error in (a) x direction, (b) y direction, (c) z direction, and (d) orientation error.

symmetric positive definite inertia matrices  $\mathcal{P}(4)$  was further developed, ensuring bounded and physically consistent parameter estimation. Theoretical results established exponential stability and semi-global uniformly ultimate boundedness of overall system without and with parametric uncertainties, respectively. Numerical simulations on a heavy-duty 4R redundant manipulator demonstrated improved convergence speed and smoother orientation responses compared to existing modular and geometric controllers, as well as robustness to significant inertial uncertainties. Future work will focus on experimental validation on large-scale manipulators and extension of the proposed framework to contact-rich and hybrid dynamical tasks.

## REFERENCES

[1] F. Bullo and R. M. Murray, "Proportional derivative (pd) control on the euclidean group," California Institute of Technology, CDC

Technical Report 95-010, 1995, available electronically via <https://www.cds.caltech.edu/~murray/preprints/cds95-010.pdf>.

[2] T. Lee, M. Leok, and N. H. McClamroch, "Geometric tracking control of a quadrotor uav on se (3)," in *49th IEEE conference on decision and control (CDC)*. IEEE, 2010, pp. 5420–5425.

[3] J. Seo, N. P. S. Prakash, A. Rose, J. Choi, and R. Horowitz, "Geometric impedance control on se (3) for robotic manipulators," *IFAC-PapersOnLine*, vol. 56, no. 2, pp. 276–283, 2023.

[4] J. Seo, N. P. Prakash, X. Zhang, C. Wang, J. Choi, M. Tomizuka, and R. Horowitz, "Contact-rich se (3)-equivariant robot manipulation task learning via geometric impedance control," *IEEE Robotics and Automation Letters*, vol. 9, no. 2, pp. 1508–1515, 2023.

[5] T. Lee and F. C. Park, "A geometric algorithm for robust multibody inertial parameter identification," *IEEE Robotics and Automation Letters*, vol. 3, no. 3, pp. 2455–2462, 2018.

[6] T. Lee, P. M. Wensing, and F. C. Park, "Geometric robot dynamic identification: A convex programming approach," *IEEE Transactions on Robotics*, vol. 36, no. 2, pp. 348–365, 2019.

[7] T. Lee, J. Kwon, and F. C. Park, "A natural adaptive control law for robot manipulators," in *2018 IEEE/RSJ International Conference on Intelligent Robots and Systems (IROS)*. IEEE, 2018, pp. 1–9.

[8] G. Alcan, F. J. Abu-Dakka, and V. Kyriki, "Constrained trajectory optimization on matrix lie groups via lie-algebraic differential dynamic programming," *Systems & Control Letters*, vol. 204, p. 106220, 2025.

[9] W.-H. Zhu, *Virtual decomposition control: toward hyper degrees of freedom robots*. Springer Science & Business Media, 2010, vol. 60.

[10] W.-H. Zhu and G. Vukobich, "Virtual decomposition control for modular robot manipulators," *IFAC Proceedings Volumes*, vol. 44, no. 1, pp. 13 486–13 491, 2011.

[11] J.-P. Humaloja, J. Koivumäki, L. Paunonen, and J. Mattila, "Decentralized observer design for virtual decomposition control," *IEEE Transactions on Automatic Control*, vol. 67, no. 5, pp. 2529–2536, 2021.

[12] J. Koivumäki, J.-P. Humaloja, L. Paunonen, W.-H. Zhu, and J. Mattila, "Subsystem-based control with modularity for strict-feedback form nonlinear systems," *IEEE Transactions on Automatic Control*, vol. 68, no. 7, pp. 4336–4343, 2022.

[13] M. Hejrati and J. Mattila, "Physical human–robot interaction control of an upper limb exoskeleton with a decentralized neuroadaptive control scheme," *IEEE Transactions on Control Systems Technology*, vol. 32, no. 3, pp. 905–918, 2023.

[14] J. Koivumäki and J. Mattila, "Stability-guaranteed force-sensorless contact force/motion control of heavy-duty hydraulic manipulators," *IEEE Transactions on Robotics*, vol. 31, no. 4, pp. 918–935, 2015.

[15] M. Hejrati and J. Mattila, "Impact-resilient orchestrated robust controller for heavy-duty hydraulic manipulators," *IEEE/ASME Transactions on Mechatronics*, 2025.

[16] S. Teng, W. Clark, A. Bloch, R. Vasudevan, and M. Ghaffari, "Lie algebraic cost function design for control on lie groups," in *2022 IEEE 61st Conference on Decision and Control (CDC)*. IEEE, 2022, pp. 1867–1874.

[17] R. M. Murray, Z. Li, and S. S. Sastry, *A mathematical introduction to robotic manipulation*. CRC press, 2017.

[18] R. Featherstone, *Rigid body dynamics algorithms*. Springer, 2008.

[19] F. C. Park, J. E. Bobrow, and S. R. Ploen, "A lie group formulation of robot dynamics," *The International journal of robotics research*, vol. 14, no. 6, pp. 609–618, 1995.

[20] T. LEE, "Geometric methods for dynamic model-based identification and control of multibody systems," Ph.D. dissertation, Department of mechanical and Aerospace Engineering, Seoul National University, 2019.

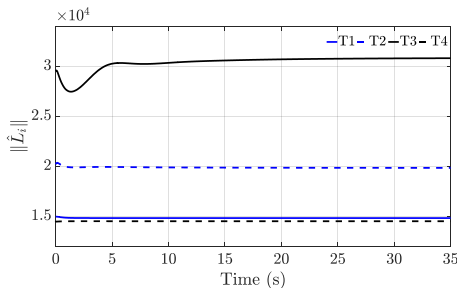


Fig. 7. Time history of the norm of the estimated parameters.